Structural Optimization 7, 55–60 © Springer-Verlag 1994

Multilevel optimization of laminated composite structures

A.V. Soeiro, C.A. Conceição António and A. Torres Marques

Faculdade de Engenharia da Universidade do Porto, Rua dos Bragas, P-4099 Porto Codex, Portugal

Abstract A two-stage optimization method aiming at the optimal design of shells and plates made of laminated composites has been developed. It is based on a mixture of sensitivity analysis, optimality criteria and mathematical programming techniques. The design variables are the optimality criteria and mathematical programming techniques. The design variables are the macro-element thicknesses and the layers' angles. Weight minimization with material efficiency maximization are the objectives with constraints on stresses and displacements. Maximization of the material efficiency is performed at one level using the conjugated method applied to the angles of the macro-element layers keeping the thicknesses constant. The other level is dedicated to weight reduction using optimality criteria and using as variables the macro-element thicknesses with the angles of the macro-element layers constant.

1 Problem definition

Methods usually employed in structural optimization have frequently faced implementation difficulties and efficiency gaps when applied to composite materials. Some possible causes are the number of design variables and constraints that may become very large. Several researchers have intended to solve the problem while developing multilevel optimization algorithms based on substructuring techniques (e.g. Schmit and Mehrinfar 1981; Watkins 1986; Weiji and Boohua 1987; Sadr *et al.* 1989).

The present work uses decomposition techniques to address the problem at two levels expecting a global efficiency improvement based on the size reduction for each stage. The types of structures studied were plates and shells, which are the most common in laminated composite materials.

The plate and shell structural analysis is carried out using the finite element displacement method. The element type adopted is the tridimensional degenerated shell element considering material anisotropy and structural layout of the layer. It is an isoparametric element with eight nodes and five degrees of freedom per node (Fig. 1) based on the Mindlin shell theory.

2 Problem formulation

Taking advantage of substructuring techniques, each structure is divided into macro-elements. The number and shape of the macro-elements are defined when elaborating the structural model and depend mainly on the degree accuracy of the analysis. All members of each macro-element have the same characteristics, such as thickness, number of layers and stacking sequence, and thickness continuity is imposed at the macro-element boundaries.

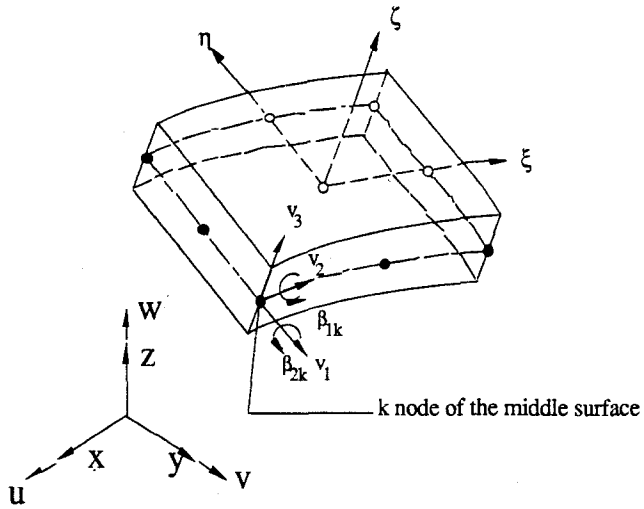

Fig. 1. Nodal parameters of the degenerated shell element

The design variables are the macro-element thickness, t_m, and the fiber layer angles, $\theta_{i,m}$, $i = 1, \ldots, N_m$, where N_m is the number of layers of the macro-element. The stacking sequence is an implicit variable since there is independency between the fiber angles of the different layers.

The objective function is the weight of the structure, assuming that the total thickness is not significant compared with the other shell or plate dimensions,

$$W(\mathbf{t}) = \sum_{k=1}^{M} \Omega_k \rho_k t_k \,, \tag{1}$$

where M is the number of macro-elements, Ω_k the average macro-element superficial area and ρ_k the specific weight of the k-th macro-element. The adopted constraints are imposed limits on layer stresses, based on the failure criteria, and on global displacements. The stress constraints have the following form:

$$g_j = 1 - \frac{R_j}{R_0} \leq 0 \,, \quad j = 1, \ldots, N_s \,, \tag{2}$$

where R_j is the strength parameter, calculated as the ratio between the failure stress and the actual stress, R_0 is a safety factor and N_s is the number of stress constraints.

The strength parameter R_j is a function of the actual stresses and is obtained using the interactive quadratic failure criteria of Tsai-Wu (Tsai and Hahn 1980; Tsai 1987),

$$[F_{ik}\sigma_i\sigma_k]\, R_j^2 + [F_{ik}\sigma_i]\, R_j = 1 \,, \tag{3}$$

where i and k take the values 1, 2 and 6, and R_j is the ratio between the maximum allowable stress and the actual stress

correspondent to the ply j.

The displacement constraints are expressed by

$$g_j = \frac{u_r}{u_0} - 1 \leq 0\,, \quad j = 1, \ldots, N_d\,, \tag{4}$$

where u_r is the global displacement r, and u_0 is the absolute maximum allowable displacement and N_d is the number of displacement constraints.

The final formulation of the present structural optimization is

$$\min\ W(\mathbf{t}),$$

$$\text{subject to } g_j(\theta, \mathbf{t}) \leq 0\,, \quad j = 1, \ldots, N_d + N_s\,, \tag{5}$$

where θ is the vector of layer angles and $\mathbf{t}$ the vector of macro-element thicknesses.

3 Optimization algorithm

The strategy adopted was to decompose the optimization algorithm in two levels. These suboptimization problems were chosen as possibly independent stages aiming at dealing with two reduced subproblems and the optimal solution is searched for by iterating between the two levels.

The first level is dedicated to maximizing the material efficiency using only the layer angles as variables. The second level consists of minimizing the weight considering the layer thicknesses as variables. In effect, the weight function does not vary with the layer angles, which affect only the constraints.

The formulation for the first level is

$$\min\ \mathrm{F}\,(\theta) \;=\; \min \overline{g}\,(\theta, \mathbf{t_0}) =$$

$$\min\left[\max\,(g_j\,, \quad j = 1, \ldots, N_d + N_s)\right]\,, \tag{6}$$

where the minimization of $F(\theta)$ is an unconstrained problem and $\mathbf{t_0}$ is the thickness vector kept constant during this suboptimization level. At this level, the changes of the layer angles create modifications of stress and displacement fields. If the initial solution is not feasible, at the end of this level, it will be closer to, or inside, the feasible region. On the other hand, if it is feasible, then at the end of this level it will be a better design.

The second level may be stated as

$$\min\ \mathrm{W(t)},\ \text{subject to } g_j(\theta_o, \mathbf{t}) \leq 0\,,\ j = 1, \ldots, N_d + N_s\,, \tag{7}$$

where the variables are only the macro-element thicknesses and the layer angles are kept constant. At this level, it is intended to minimize the weight and bring the value of at least one of the constraints close to zero.

The optimization techniques are different for each level such that at the first level, the conjugate gradient method was adopted and at the second level an optimality criterion was chosen. For both levels, the sensitivity analysis was evaluated using the adjoint structure method. The conjugate gradient method of the first level used was that presented by Polak and Ribiere (1971). The algorithm is stopped if any of the global convergence conditions, C_1 or C_2, are verified or if the number of cycles exceeds a control parameter I_3. The optimization sequence may be graphically represented, as shown in Fig. 2, and the basic flowchart is presented in Fig. 3.

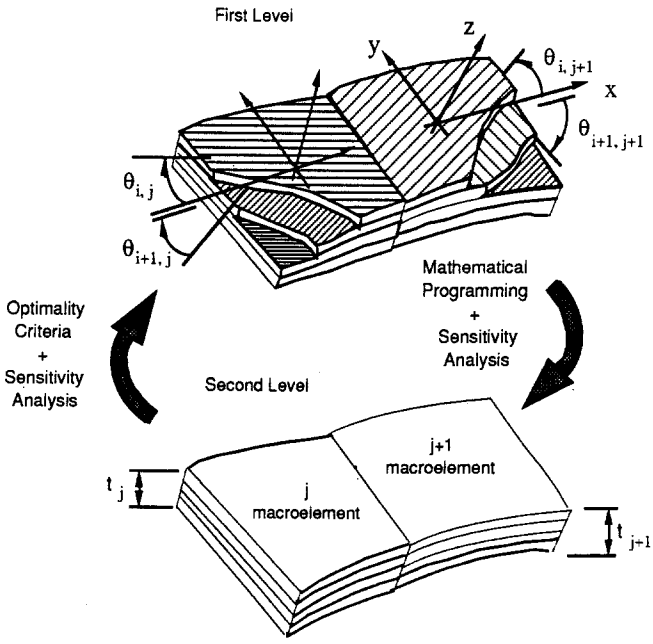

Fig. 2. Representation of the optimization sequence

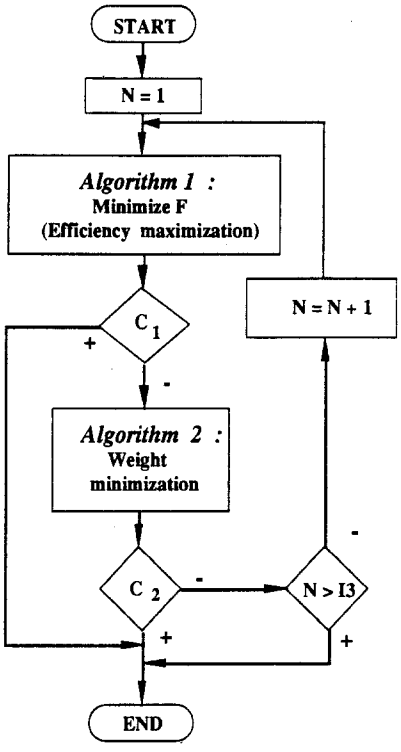

Fig. 3. Flowchart of the optimization method

The optimality criteria were developed based on the optimality condition that the constraint with the greater value becomes active,

$$\overline{g} = 0\,. \tag{8}$$

Indeed it was considered that the absolute value of the constraint with the greater value is decreased during the iteration history. This is represented by

$$\alpha^k = \frac{\overline{g}^{k+1}}{\overline{g}^k} \leq 1, \tag{9}$$

where α^k sets the step to decrease the absolute constraint value. If the approximation

$$\frac{\overline{g}^{k+1} - \overline{g}^k}{t_j^{k+1} - t_j^k} \approx \frac{\mathrm{d}\overline{g}^k}{\mathrm{d}t_j^k} \tag{10}$$

is considered together with the adopted optimality condition, then

$$t_j^{k+1} = \beta_j^k t_j^k, \tag{11}$$

with

$$\beta_j^k = 1 + \frac{\overline{g}^k}{\dfrac{\mathrm{d}\overline{g}^k}{\mathrm{d}t_j^k} t_j^k} \left(\alpha^k - 1\right), \quad j = 1, \ldots, M, \tag{12}$$

where $\overline{g}^k$ is the constraint with the maximum value in iteration k, $\dfrac{\mathrm{d}\overline{g}^k}{\mathrm{d}t_j^k}$ is the gradient of the constraint with the maximum value relative to the thickness variable t_j and M is the number of macro-elements.

The scalar α^k is obtained by linear search through minimization of the function $Q = \overline{g}^2$, and then:

$$\alpha^k = 1 - \left(M + \frac{\overline{g}^k}{M} \sum_{i,j=1}^{M} \frac{\dfrac{\mathrm{d}^2\overline{g}^k}{\mathrm{d}t_i \mathrm{d}t_j}}{\dfrac{\mathrm{d}\overline{g}^k}{\mathrm{d}t_i} \dfrac{\mathrm{d}\overline{g}^k}{\mathrm{d}t_j}} \right)^{-1} \tag{13}$$

where $\dfrac{\mathrm{d}^2\overline{g}^k}{\mathrm{d}t_i \mathrm{d}t_j}$ are the components of the Hessian matrix.

The convergence condition chosen for the algorithm during and at the end of the first level was based on the absolute variation criterion since the objective function F has values close to zero. Convergence conditions were defined for the algorithm at the second level, during and at the end of the cycle, based on the relative variation criterion due to the significant values of the weight function.

4 Examples

The performance of the proposed algorithm when applied to two different structures having several initial conditions is studied here. The first example is a cylindrical shell subjected to concentrated loads and the second is a skewed plate loaded uniformly in the direction perpendicular to the middle plane.

Table 1. Material properties of composite layers

Elastic constants		Values	Mechanical strength		Values
Elastic modulus (GPa)	E_1	206.84	Longitudinal (MPa)		
	E_2	5.17	tensile	X	760
			compression	X'	760
Shear modulus (GPa)	G_{12}	3.1			
	G_{13}	2.586	Transversal (MPa)		
	G_{23}	2.586	tensile	Y	30
			compression	Y'	30
Poisson's coefficients	ν_{12}	0.25			
	ν_{13}	0.25	Shear (MPa)	S	70
	ν_{23}	0.25			

The elastic and mechanical properties of the material layers of both structures are presented in Table 1 and the specific

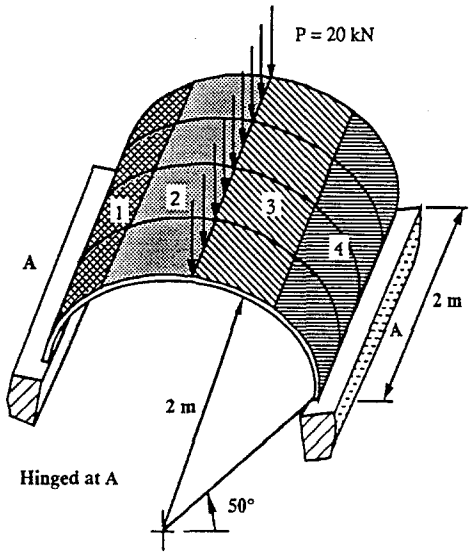

a) Full structure, four macroelements

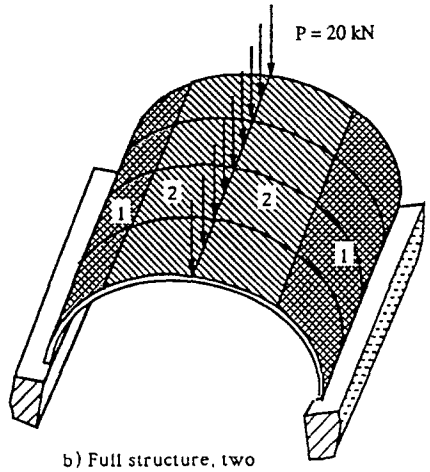

b) Full structure, two macroelements

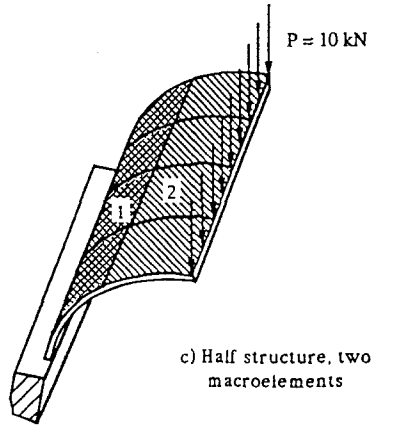

c) Half structure, two macroelements

Fig. 4. Structural models of the first structure

weight is $\rho = 2{,}1 \times 10^3$ kg/m^3. It was considered that the laminated material has five layers.

The geometric definition of the cylindrical shell with vertical discrete loads along the symmetry plane is presented

in Fig. 4. The stress constraints are defined with a safety factor of $R_0 = 2$ and the displacement constraints have an absolute maximum of $u_0 = 0.05$ m. The example was substructured in three different arrangements that were tested and the respective algorithm performance was analysed.

The first substructuring consisted of the division into four equal macro-elements, as shown in Fig. 4a. The solution of the optimization method is presented in Table 2. The initial solution was infeasible and after the first algorithm level the constraints were satisfied using only the redistribution of the angles of the layers. It is worth noting that if the thicknesses were kept constant the feasible weight would be twice the initial one (Antônio 1991).

Table 2. Results for Case a in Fig. 2 (t_i in mm)

Macro	Variable	Initial solution	Final solution
1	t_1	20.000	8.245
	θ_1	30°	81.2°
	θ_2	-30°	-58.6°
	θ_3	30°	30.4°
	θ_4	-30°	-42.5°
	θ_5	30°	83.5°
2	t_2	20.000	11.112
	θ_6	30°	61.7°
	θ_7	-30°	-55.3°
	θ_8	30°	33.7°
	θ_9	-30°	-75.6°
	θ_{10}	30°	84.0°
3	t_3	20.000	12.865
	θ_{11}	30°	59.6°
	θ_{12}	-30°	-61.6°
	θ_{13}	30°	36.0°
	θ_{14}	-30°	-77.4°
	θ_{15}	30°	86.9°
4	t_4	20.000	7.920
	θ_{16}	30°	81.5°
	θ_{17}	-30°	-60.9°
	θ_{18}	30°	29.2°
	θ_{19}	-30°	-40.7°
	θ_{20}	30°	83.7°
Weight (kg)		235.738	118.058
CPU (s)			906

The second arrangement of the macro-elements consisted of two symmetrical macro-elements with the symmetry plane containing the loads normal to the shell. The initial solution was the same as the first run and the corresponding optimization results are presented in Table 3.

The third division of the structure to macro-elements was to consider half the structure, obtained by cutting the structure by the symmetry plane and the expected symmetry of the solution was guaranteed with adequate boundary conditions. The algorithm was tested with four initial designs and the results are presented in Table 4.

The optimized solutions are different for all six runs. The maximum absolute variation of the weight between the solutions is 2.982 kg and the maximum relative variation of the weight verified is 2.6%.

Table 3. Results for Case b in Fig. 2 (t_i in mm)

Macro	Variable	Initial solution	Final solution
1	t_1	20.000	7.707
	θ_1	30°	85.6°
	θ_2	-30°	-52.2°
	θ_3	30°	29.9°
	θ_4	-30°	-41.2°
	θ_5	30°	87.9°
2	t_2	20.000	11.760
	θ_6	30°	62.7°
	θ_7	-30°	-54.0°
	θ_8	30°	55.4°
	θ_9	-30°	-72.2°
	θ_{10}	30°	89.7°
Weight (kg)		235.738	116.642
CPU (s)			679

The second structure studied using the algorithm has a larger number of design variables (18) and an unsymmetric shape as shown in Fig. 5. The stress constraints were defined with a safety coefficient of $R_0 = 4$ and the displacement constraints were evaluated with an absolute maximum displacement of $u_0 = 0.075$ m. The model substructuring consisted of the division into three macro-elements distributed along the structure.

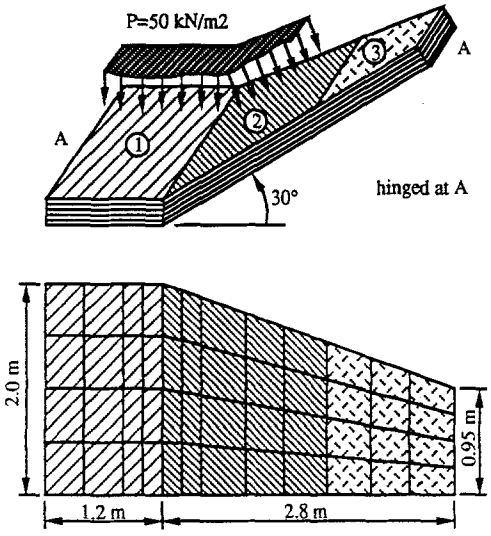

Fig. 5. Geometrical definition, load conditions and boundary conditions of the skew plate

The optimization results, presented in Table 5, comprise two different initial conditions classified as Case 1 and Case 2. The final design presents an absolute variation of the weight of 0.990 kg and a relative variation of the weight of 0.2%. The differences in CPU time may be explained by the choice of more adequate layer angles, resulting in different iteration paths.

5 Final considerations

It is evident that the choice of a strategy based on the creation of two separate suboptimization problems produced a robust method for the cases studied. In effect, the various runs with

Table 4. Results for Case c in Fig. 2 (t_i in mm)

Macro	Variable	Initial solution				Final solution			
		Case 1	Case 2	Case 3	Case 4	Case 1	Case 2	Case 3	Case 4
1	t_1	20.000	20.000	30.000	30.000	7.498	7.376	4.284	7.627
	θ_1	0°	-75°	-75°	30°	84.4°	-84.8°	-88.3°	87.5°
	θ_2	-45°	75°	75°	-30°	−78.4°	75.7°	73.9°	-52.5°
	θ_3	-30°	-75°	-75°	30°	-41.2°	-73.3°	-73.3°	30.0°
	θ_4	0°	75°	75°	-30°	2.1°	78.8°	77.9°	-44.1°
	θ_5	20°	-75°	-75°	30°	90.2°	-85.6°	-89.6°	89.5°
2	t_2	20.000	20.000	30.000	30.000	12.048	12.118	15.014	11.859
	θ_6	45°	25°	25°	30°	69.8°	71.1°	73.1°	65.7°
	θ_7	-60°	-25°	-25°	-30°	-39.3°	-42.0°	-37.4°	-43.9°
	θ_8	0°	25°	25°	30°	-4.1°	26.1°	28.5°	59.0°
	θ_9	70°	-25°	-25°	-30°	83.0°	-12.4°	-18.0°	-73.7°
	θ_{10}	-10°	25°	25°	30°	-85.6°	81.2°	92.4°	81.7°
Weight (kg)		235.738	235.738	353.607	353.607	117.911	117.687	119.624	117.315
CPU (s)						511	324	344	678

different initial conditions produced designs with very close values. This fact was confirmed by re-running the examples with the final optimized solutions without further significant enhancements.

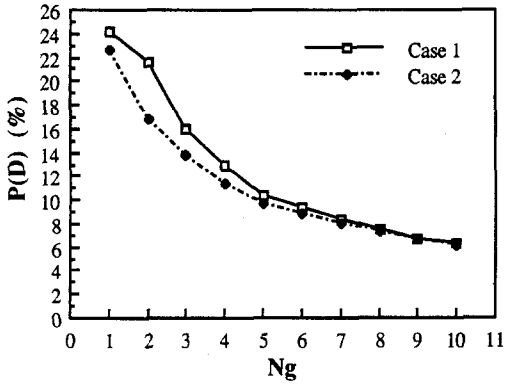

Fig. 6. Probability that a constraint selected in the set constraints with greater values could become the maximum constraint

The choice of the objective function at the first level as the value of the maximum constraint was adequate to find a better distribution of the layer angles. In fact, since this update function is a structural response estimator to the prescribed limits, based on energetic formulations due to the evaluation of the stress and displacement fields, the corresponding decrease imposes a minimization of the potential energy. The analysis of the iteration history of this estimator shows that it is not affected by the nature of the constraint, stress or displacement, guaranteeing a convergence stability. In effect, the results show small deviations of the objective function along the process caused by the location change of the constraint.

Another conclusion was obtained from the analysis made to verify the adequacy of using a single constraint instead of a multi-objective function including the constraints with greater values. The procedure consisted of verifying, for the skewed plate, the chance that any constraint from the set of constraints N_g could become the one with the maximum value. The results are shown graphically in Fig. 6 with a set varying from one to ten constraints. It was noted that

Table 5. Results (t_i in mm)

Macro	Variable	Initial solution		Final solution	
		Case 1	Case 2	Case 1	Case 2
1	t_1	60.000	60.000	22.836	27.969
	θ_1	-75°	-45°	-84.3°	-87.0°
	θ_2	75°	45°	76.3°	63.1°
	θ_3	-75°	-45°	-75.2°	-41.4°
	θ_4	75°	45°	76.6°	65.0°
	θ_5	-75°	-45°	-86.8°	-94.8°
2	t_2	60.000	60.000	33.968	35.800
	θ_6	-30°	-60°	-78.3°	-89.3°
	θ_7	30°	60°	71.1°	60.7°
	θ_8	-30°	-60°	-33.5°	-54.6°
	θ_9	30°	60°	67.7°	67.8°
	θ_{10}	-30°	-60°	-90.8°	-87.2°
3	t_3	60.000	60.000	50.285	40.016
	θ_{11}	-45°	-20°	-77.6°	-90.6°
	θ_{12}	45°	20°	56.8°	69.7°
	θ_{13}	-45°	-20°	-55.3°	-40.1°
	θ_{14}	45°	20°	80.7°	80.7°
	θ_{15}	-45°	-20°	-122.3°	-116.3°
Weight (kg)		905.740	905.740	515.588	516.578
CPU (s)				4372	6975

the probability decreases almost exponentially with the set dimension and there is no need to consider more than one constraint at the first level due to the increased sensitivity analysis work without apparent benefit.

The final conclusion is that while suboptimizing there is an increase in software programming that is paid off by the robustness due to the separation of the variables. It should be emphasized that the variable separation could become beneficial when there are preassigned integer layer angles, as is frequent in most production lines. In any case, the procedure seems adequate for a predesign phase that may be followed by a more accurate analysis if more precision is needed.

References

António, C. 1991: *Multilevel optimization of laminated composite structures.* M.Sc. Thesis, Universidade do Porto

Polak, E. 1971: *Computational methods in optimization.* New York: Academic Press

Sadr, H.; Afzali, M.; Sabzevari, H. 1989: Calcul et optimisation des structures composites stratifiées. *Rapport CETIM Senlis*

Schmit, L.A.; Mehrinfar 1982: Multilevel optimum design of structures with fiber–composite stiffened–panel components. *AIAA J.* **20**, 138-147

Soeiro, A.; António, C.; Marques, T. 1991: Multilevel optimization of laminated composite structures. Poster presented at NATO ASI, *Optimization of Large Structural Systems* (held in Berchtesgaden, Germany)

Tsai, S.W.; Hahn, H.T. 1980: *Introduction to composite materials.* Westport, Connecticut: Technomic Publishing

Tsai, S.W. 1987: *Composites design.* Dayton: Think Composites

Watkins, R.I. 1986: Multilevel optimization of composite structures. *Composite Structures* 4, 1.393-1.403

Weiji, L.; Boohua, S. 1987: Multilevel optimization procedure of composite structures. *Composites Structures* 4, 1.357-1.367

Received Feb. 18, 1992
Revised manuscript received Mar. 23, 1993